



A versatile cobalt catalyst for the reductive amination of carbonyl compounds with nitro compounds by transfer hydrogenation



Peng Zhou^a, Zehui Zhang^{a,*}, Liang Jiang^a, Changlin Yu^b, Kangle Lv^a, Jie Sun^a, Shuguo Wang^a

^a Key Laboratory of Catalysis and Materials Sciences of the Ministry of Education, South-Central University for Nationalities, Wuhan, 430074, PR China

^b School of Metallurgy and Chemical Engineering, Jiangxi University of Science and Technology, 86 Hongqi Road, Ganzhou, 341000, PR China

ARTICLE INFO

Article history:

Received 10 February 2017

Received in revised form 26 March 2017

Accepted 7 April 2017

Available online 8 April 2017

Keywords:

Non-noble heterogeneous catalyst

Nitro compounds

Hydrogenation

Transfer hydrogenation

Reductive coupling reaction

ABSTRACT

Co nanoparticles embedded in mesoporous nitrogen-doped carbon (abbreviated as Co@CN-800) were prepared and found to be resistant to acid. The Co@CN-800 catalyst was found to be active and selective for the one-pot reductive amination of carbonyl compounds with nitro compounds by transfer hydrogenation with formic acid as the hydrogen donor, affording the corresponding secondary amines with excellent yields (89.6–99%). Both nitrogen atoms and Co nanoparticles were of great importance in the one-pot reductive amination over the Co@CN-800 catalyst by formic acid, and the protic N-H⁺ and hydridic Co-H⁻ were proposed to be the active species for the transfer hydrogenation reactions. Furthermore, the Co@CN-800 catalyst was highly stable without loss of its activity.

© 2017 Elsevier B.V. All rights reserved.

1. Introduction

Catalytic hydrogenation represents a fundamental methodology in the chemical industry [1–4]. Nitro compounds are one of the most readily available and valuable starting materials in organic synthesis [5]. Nitro compounds are majorly used for the production of primary amines and their derivatives such as secondary and tertiary amines with wide applications [6–9]. Secondary amines are generally synthesized by amine-carbonyl reductive amination [10], direct alkylation of amines with alkyl halides [11], Buchwald-Hartwig [12,13] and Ullman-type carbon-nitrogen cross-coupling reactions [14,15], as well as the direct *N*-alkylation of amines with alcohols [16]. Among them, the amine-carbonyl reductive amination method is preferable, because of the readily availability of the substrates, high atom-economy and environmentally friendly.

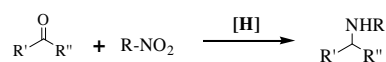
Reductive amination mainly employs primary amines as the substrates, which are usually prepared in advance by the hydrogenation of nitro compounds. Obviously, it is highly attractive to perform the one-pot reductive amination of carbonyl compounds with nitro compounds by avoiding intermediate separation, purifications steps, and minimizing energy. There have been a few reports on the one-pot reductive amination, mainly over noble

metal catalysts with H₂ as the hydrogen source (Scheme 1, Method A) [17–22]. These methods demonstrated several drawbacks such as the limited substrate scope and low selectivity. Of particular note is that harsh conditions were applied for non-noble metal catalysts. For example, carbon-supported iron oxide catalyst produced 45–91% yields of secondary amines within 30 h at 170 °C and 70 bar H₂ [17]. Obviously, these processes are constrained by the need of specialized equipment and potential safety issues regarding H₂ handling.

Currently, catalytic transfer hydrogenation has received a considerable interest, which uses other hydrogen donors in replacement of H₂ [23]. One-pot reductive amination by transfer hydrogenation has been reported to perform with CO [24,25] and formic acid as the hydrogen donors over noble metal catalysts (Scheme 1, Method B & C) [26–28]. The use of CO at high pressure still encounters the problems with H₂ as discussed above [24,25]. Formic acid, a natural biomass-derivative and also accessible via CO₂ reduction, represents an economical, safe and easy-to-handle liquid hydrogen carrier for transfer hydrogenation [29]. Unfortunately, its application in the one-pot reductive amination has been rarely developed [26–28]. All the reported methods were used noble metal catalysts, and an additive such as base was generally required [27,28]. Therefore, it is highly demanded to develop efficient and economic methods with non-noble metal catalysts for this reaction.

* Corresponding author.

E-mail address: zehuizh@mail.ustc.edu.cn (Z. Zhang).



Method	Catalyst	Hydrogen donors
A	Noble/Non-noble metal	H ₂
B	Noble metal	CO/CO-H ₂ O
C	Noble metal	HCOOH/HCOOH-base
This work	Heterogeneous Co catalyst	HCOOH

The present work on the use of non-noble metal catalyst with formic acid.

Scheme 1. Current methods for the one-pot synthesis of secondary amines.

Unlike the noble metal catalysts such as supported Pd and Au, non-noble metal catalysts not only have intrinsic low catalytic activity, but also they can react with formic acid, limiting their application in the transfer hydrogenation with formic acid as the hydrogen donor. In recent years, nitrogen-containing carbon based non-noble metal catalysts been intensively studied for the electrochemical oxygen reduction reaction (ORR) [30–32]. Some of them showed comparable or even superior activity to the conventional Pt/C catalyst, because the incorporation of nitrogen atoms in the carbon structure can enhance their chemical, electrical, and functional properties. Currently, the use of nitrogen-doped carbon based earth abundant non-noble metal catalysts has received great attention for a variety of organic redox transformations [33–35], showing great potential for replacing expensive noble-metal-based catalysts. ZIF-67 (ZIF indicates zeolitic imidazolate framework) is one of the most investigated metal organic frameworks (MOFs), that is an emerging class of ordered porous materials built with metal cobalt cations and 2-methylimidazole anions [36]. Owing to their high surface area, porosity, and chemical tunability, ZIF-67 has shown great potential for applications in a wide range of fields such as catalysis, luminescence, gas storage, and separation. ZIF-67 has recently received great interest in the preparation of new metal oxides or carbon nanomaterials by thermal decomposition. One of the main obstacle for the use of base metal catalysts towards the transfer hydrogenation with formic acid as the hydrogen donor is that the base metal based catalyst reacted with formic acid. To overcome this issue, the addition of base was required for the transfer hydrogenation with formic acid. For example, M. Beller and co-worker studied the transfer hydrogenation of nitroarenes with formic acid over the CoO_x/NC catalyst, but the base Et₃N was required [37]. Recently, some researchers discovered that non-noble metal nanoparticles embedded into carbon structure were stable and resistant to acid [38]. For organic transformation, heterogeneous catalysts with high surface area and large pore volume benefited the mass transfer of organic molecules. Following this thought, mesoporous nitrogen-doped carbon-embedded Co catalysts (Co@CN) were prepared by the one-step pyrolysis of ZIF-67 with silica as the hard template, followed by the acid-leaching to wash off silica and surface Co nanoparticles that loosely bonded on the surface of the nitrogen-doped carbon material. The as-prepared catalysts were resistant to acid, and were used for the one-pot reductive amination by transfer hydrogenation with formic acid as the hydrogen donor for the first time.

2. Experimental section

2.1. Materials

All of the solvents were purchased from Sinopharm Chemical Reagent Co., Ltd. (Shanghai, China). All of the chemicals were purchased from Aladdin Chemicals Co. Ltd. (Beijing, China). 95 wt.% DCOOH in 5 wt. D₂O was purchased from the J&K Chemical Co. Ltd., (Beijing, China). LUDOX[®] HS-40 colloidal silica (40 wt.% in H₂O) was purchased from Sigma-Aldrich (St Louis, USA).

2.2. Catalyst preparation

2-Methylimidazole (5.5 g) was firstly dissolved in 20 mL of water, and then 1 mL of 40 wt.% colloidal silica was added. Then the mixture was magnetically stirred at room temperature for 1 h. To this mixture, Co(NO₃)₂·6H₂O (0.45 g) in 3 mL of water was added dropwise. After the addition of Co(NO₃)₂ solution, the mixture was continuously stirred at 25 °C for another 6 h. The resulting purple precipitates were obtained via centrifugation and washed with water and methanol for twice, respectively, and finally dried in a vacuum oven to get the ZIF-67/SiO₂ composite.

The ZIF-67/SiO₂ composite (2.0 g) was pyrolyzed at three representative temperatures (600, 800 or 900 °C) for 8 h in a nitrogen atmosphere at a heating rate of 1 °C/min from room temperature. The as-prepared materials were denoted as Co/CN-SiO₂-T, where T represents the pyrolysis temperature. Then the Co/CN-T samples were treated with 20 wt.% HF for 12 h at room temperature, and then washed with water to pH = 7. The as-made catalysts were labeled as Co@CN-T.

2.3. Catalyst characterization

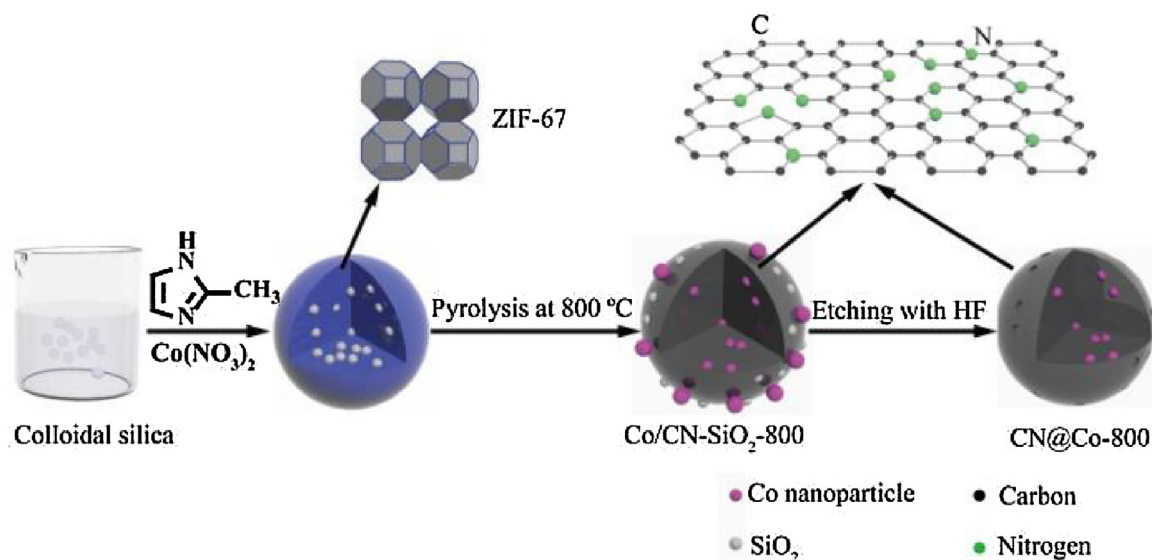
Transmission electron microscope (TEM) was performed on an FEI Tecnai G²-20 instrument. X-ray powder diffraction (XRD) measurements were conducted on a Bruker advanced D8 powder diffractometer (Cu Kα), operating with 2θ range of 10–80° at a scanning rate of 0.016°/s. X-ray photoelectron spectroscopy (XPS) experiments were carried out on a Thermo VG scientific ESCA MultiLab-2000 spectrometer with a monochromatized Al Kα source (1486.6 eV) at constant analyzer pass energy of 25 eV. The cobalt content was determined by inductively coupled atomic emission spectrometer (ICP-AES) on an IRIS Intrepid II XSP instrument (Thermo Electron Corporation). Raman spectra were measured on a confocal laser micro-Raman spectrometer (Thermo Fischer DXR) equipped with a diode laser of excitation of 532 nm (laser serial number: AJC1200566). Spectra were obtained at a laser output power of 1 mW (532 nm), and a 0.2 s acquisition time with 900 lines/mm grating (Grating serial number: AJG1200531). Nitrogen physisorption measurements were conducted at 77 K on a quantachrome Autosorb-1-C-MS instrument. Surface area was determined by the standard BET method based on the relative pressure between 0.05 and 0.20. The pore size distribution was calculated using the non-local density functional theory method.

2.4. Catalytic transfer hydrogenation of nitrobenzene

Typically, Co@CN-800 catalyst (40 mg), nitrobenzene (1 mmol), formic acid (3 mmol) and tetrahydrofuran (THF, 10 mL) were charged in a 50 mL autoclave, which was equipped with a magnetic stirrer and a temperature controller. After removal of the air in the autoclave with N₂, the autoclave was charged with 1 MPa N₂ at room temperature, then it was heated from room temperature to 110 °C within 5 min and kept at 110 °C for 10 h with a magnetic stirring at 1000 rpm. After cooling to room temperature, the mixture was diluted to a certain volume and the content of each compound was quantified based on the internal standard method using toluene as the internal standard.

2.5. Analytical methods

Products analysis was performed on an agilent 7890A gas chromatography (GC) instrument with a crosslinked capillary HP-5 column (30 m × 0.32 mm × 0.4 mm) equipped with a flame ionization detector. Operating conditions were as follows: The flow rate of the N₂ carrier gas was 40 mL min⁻¹, the injection port temperature was 300 °C. The GC oven temperature program was as follows:



Scheme 2. The process for the fabrication of the Co@CN-800 catalyst.

Table 1

The weight percentage of cobalt and atomic percentage nitrogen in the samples.

	Co/CN-SiO ₂ -800	Co@CN-600	Co@CN-800	Co@CN-900
Co wt. %	38.2 ^a	17.5	23.8	14.5
N at. %	–	26.7	6.9	3.7

^a The cobalt content was calculated after the deduction of SiO₂.

Table 2

Textural parameters of the Co@CN-T catalysts.

Catalyst	Surface area (m ² /g)	Average pore size (nm)	Pore volume (cc/g)
Co@CN-600	374.8	4.8	0.74
Co@CN-800	290.4	6.3	0.96
Co@CN-900	160.2	6.9	0.58

50 °C ramp 10 °C/min to 280 °C and the detector temperature was set to 300 °C. The content of each compound was determined based on the internal standard.

2.6. Recycling experiments

After reaction, the Co@CN-800 catalyst was collected with an external magnet, and the spent catalyst was exhaustively washed with water and ethanol, respectively. Then it was dried at 50 °C in a vacuum oven. The spent catalyst was used for the next run under the same conditions. Other cycles were repeated with the same procedure.

3. Results and discussion

3.1. Catalyst synthesis and characterization

ZIF-67 was used as the precursor for the synthesis of the catalyst. The fabrication of the Co@CN-T catalysts is schematically illustrated in Scheme 2. Silica was used as a hard template during the preparation of ZIF-67, which was formed by the coordination of Co²⁺ with 2-methylimidazole ligand. The X-ray powder diffraction (XRD) pattern of the as-made ZIF-67/SiO₂ (Fig. S1) was consistent with its standard XRD pattern of ZIF-67 [36]. In addition, there were no other peaks in the XRD patterns of ZIF-67/SiO₂, suggesting there were no other impurities. Then pyrolysis of the ZIF-67/SiO₂ composite generated the black powder (abbreviated

as Co/CN-SiO₂-T), in which T represents the pyrolysis temperature. During this process, Co²⁺ was reduced to Co nanoparticles, and the nitrogen-doped carbon support was also formed. The Co/CN-SiO₂-T samples contained two types of Co nanoparticles. Some Co nanoparticles should deposit on the surface of the carbon materials, which were washed off by the reaction with acid. While some Co nanoparticles were encapsulated or embedded in the carbon material that there were resistant to acid. The carbon layer protected the cobalt nanoparticles from acid-leaching. For example, N-doped carbon encapsulated Co₃O₄ nanoparticles were reported to be stable in acidic media [38]. Treatment of Co/CN-SiO₂-T with 20 wt.% HF could simultaneously wash off the silica template and the surface Co nanoparticles. Finally, the nitrogen-doped carbon-embedded Co nanoparticles (Co@CN-T) were obtained. It was noted that the nitrogen atomic percentage (at.%) in the Co@CN-T catalysts decreased with the increase of pyrolysis temperature (Table 1), which should be caused by a more serious breakage of the carbon-nitrogen bonds at a higher pyrolysis temperature [36]. Interestingly, the weight percentage of cobalt in the Co@CN-800 catalyst was the highest (Table 1). The possible reason was that much more Co nanoparticles were embedded at the pyrolysis temperature of 800 °C, and thus there were not washed off by acid.

Co nanoparticles were clearly observed in the TEM images of the Co@CN-T catalysts, and the average size of the Co nanoparticles were calculated to be 8.1, 9.7 and 10.3 nm for the Co@CN-600, Co@CN-800, Co@CN-900 catalysts, respectively (Fig. 1). These results suggested that a higher pyrolysis temperature caused a

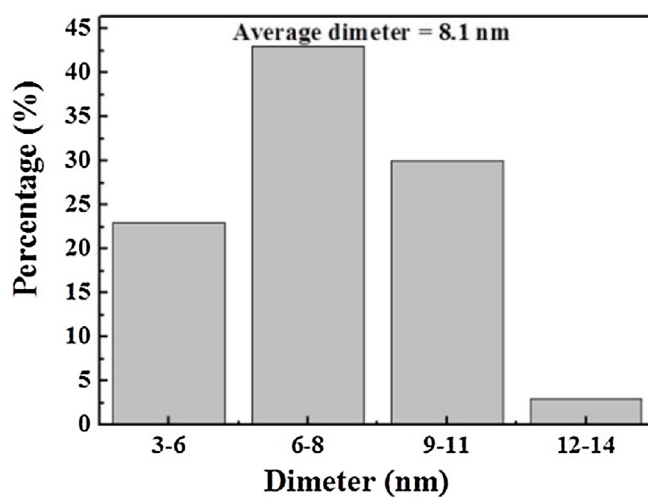
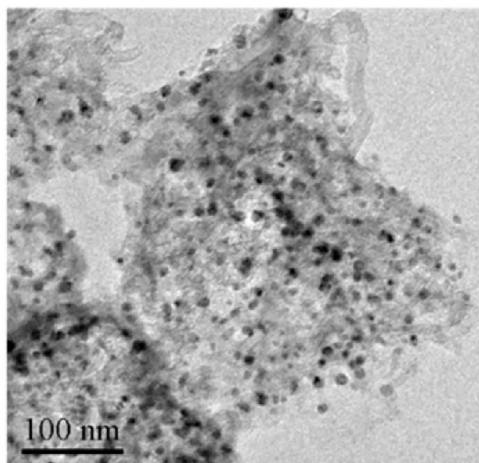
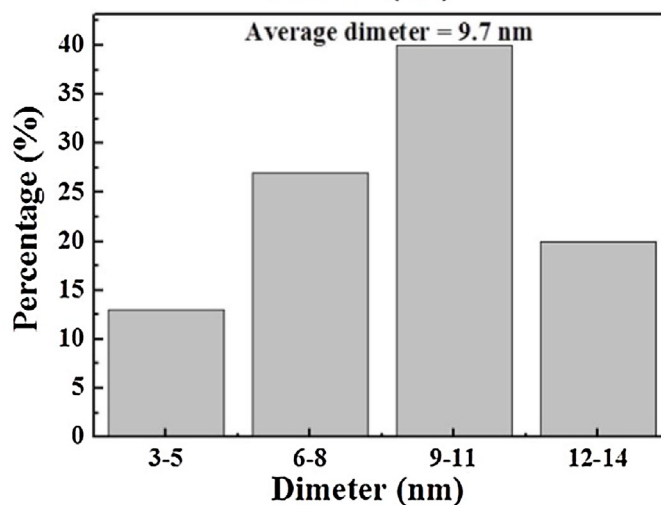
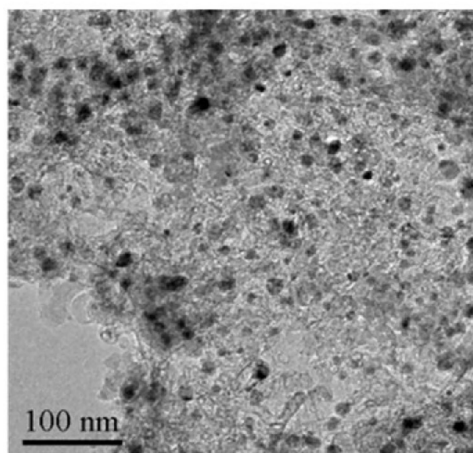
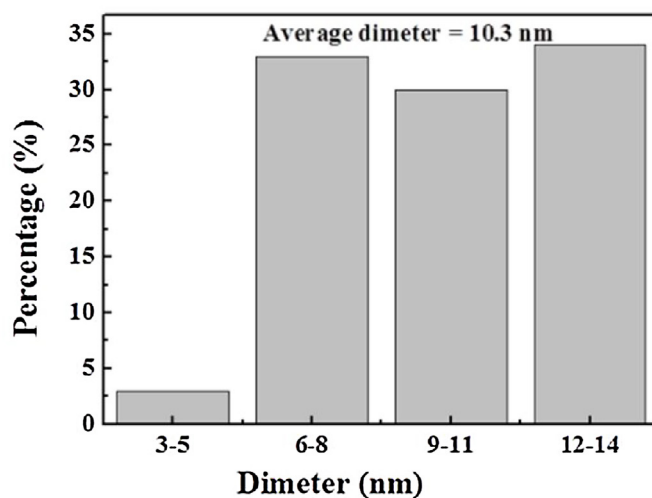
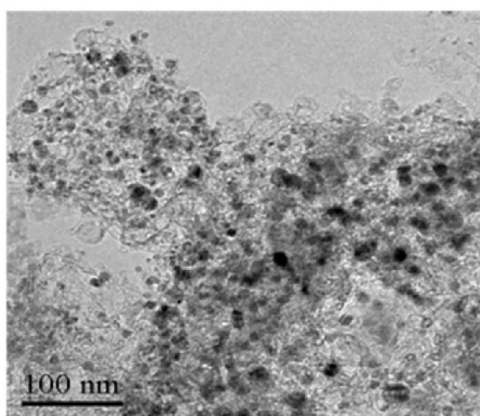
(a) Co@CN-600**(b) Co@CN-800****(c) Co@CN-900**

Fig. 1. TEM images of the Co@CN-T catalysts and the size distribution of Co nanoparticles.

growth of Co nanoparticles. Compared with the TEM image of the Co@CN-800 catalyst (Fig. 1), Co nanoparticles with a much larger size of 25.9 nm were observed on the surface of the Co/CN-SiO₂-800 sample (Fig. S2), which could be washed off by acid. Higher resolu-

tion TEM (HRTEM) image of the Co@CN-800 catalyst also revealed that Co nanoparticles were embedded in the carbon layer (Fig. S3).

In addition, porous structure was observed in the Co@CN-800 catalyst (Fig. 1), due to the removal of silica from the Co/CN-SiO₂-800 sample. Nitrogen adsorption isotherms of the Co@CN-T catalyst

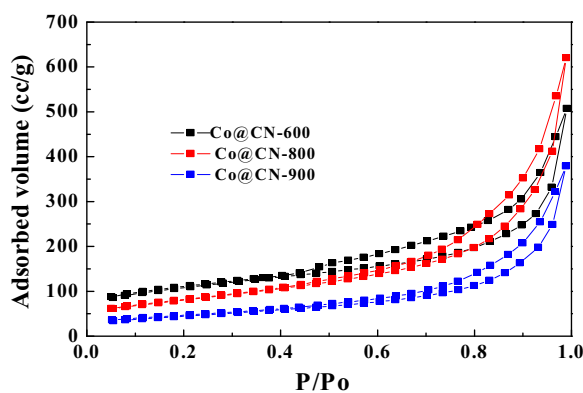


Fig. 2. Nitrogen adsorption-desorption isotherms of the Co@CN-T catalysts at 77 K.

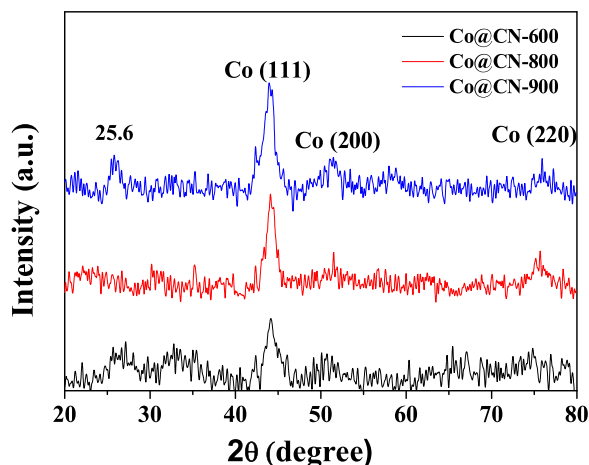


Fig. 3. XRD patterns of the Co@CN-T catalysts.

displayed a type-V curve and H3-type hysteresis loop, which is characteristic of mesoporous structure (Fig. 2). The texture parameters of the Co@CN-T catalysts are listed in Table 2. The Co@CN-800 had a medium surface area ($290.4 \text{ m}^2/\text{g}$), and the largest pore volume ($0.96 \text{ cm}^3/\text{g}$). Pore size distribution (Fig. S4) demonstrated the Co@CN-T catalysts had a wide size distribution centring around 2 nm and 6 nm. A highly porous structure in the Co@CN-T catalyst would be helpful to expose more active sites and facilitate the mass diffusion of reaction molecules.

The X-ray powder diffraction (XRD) pattern of Co/CN-SiO₂-800 presents three peaks at $2\theta = 44.1$, 51.5 and 75.8° (Fig. S5), corresponding to the (111), (200) and (220) plans of metallic Co nanoparticles (JCPDS No. 15-0806) [39]. The three peaks were also observed in the XRD pattern of Co@CN-800 (Fig. 3), but with a much weaker intensity due to the removal of surface Co nanoparticles from Co/CN-SiO₂-800 (Fig. S5). In addition, the particle size was calculated to be 7.6 and 20.8 nm by the Scherrer equation for Co@CN-800 and Co/CN-SiO₂-800, respectively, which were in agreement TEM results. Similar XRD patterns were also observed for Co@CN-600 and Co@CN-900 (Fig. 3). Besides the metallic Co peaks, a peak at 25.6° was attributed to the turbostratic ordering of the carbon and nitrogen atoms in the graphite layers (JCPDS No. 01-0646) [40]. Raman spectrum of CN@Co-800 (Fig. S6) exhibited a D peak at 1325 cm^{-1} and a G peak at 1580 cm^{-1} , which are associated with structural defects of lattice symmetry and the characteristic of the sp^2 hybridization of carbon [40]. The D band was stronger than the G band, indicating much more defects were present in the graphitic network of the Co@CN-800 catalyst.

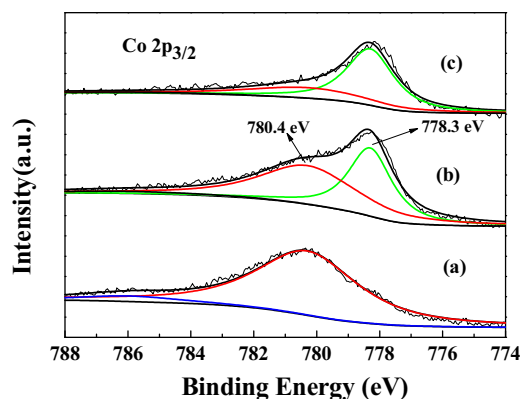


Fig. 4. XPS spectra of Co $2p_{3/2}$ for the Co@CN-T catalysts. (a) The Co@CN-600 catalyst; (b) The Co@CN-800 catalyst; (c) The Co@CN-900 catalyst.

For comparison, the Co@CN-800 catalyst was subjected to be treated in the air at 200°C for 6 h, which was abbreviated as Co@CN-800-Air. Characteristic peaks of Co_3O_4 crystalline structure (JCPDS No. 65-3103) at $2\theta = 31.4$, 36.8 , 44.7 , 55.6 , 59.2 and 65.2° were observed in the XRD pattern of Co@CN-800-Air (Fig. S7), suggesting metallic Co in Co@CN-800 was oxidized to Co_3O_4 after the treatment in the air at 200°C .

X-ray photoelectron spectroscopy (XPS) spectrum of the Co $2p_{3/2}$ peak for the Co@CN-800 catalyst could be deconvoluted into two peaks with the binding energies (BEs) around 778.3 and 780.5 eV. The binding energy at 778.3 eV was assigned to the metallic cobalt, while the binding energy at 780.5 eV was assigned to the corresponding to the oxidation state Co(+2), which indicated that the surface metallic Co was partially oxidized in the air during the storage [41]. It was different from the complete oxidation of metallic Co into Co_3O_4 in the air at 200°C for the Co@CN-800-Air catalyst. Interestingly, XPS spectra only gave a signal of the oxidation state Co for Co@CN-600, and the metallic Co peak area in Co@CN-900 was larger than that of Co@CN-800 (Fig. 4). The possible reason should be due to the fact that the surface of Co nanoparticles with a larger size was more difficult to be oxidized [42]. The N 1s XPS spectrum of the Co@CN-800 catalyst was fitted into three peaks with BEs at about 398.5, 399.5 and 400.8 eV, which were corresponded to pyridinic N (N-1), pyrrolic N (N-2) and graphitic N (N-3), respectively (Fig. 5) [39]. In addition, as shown in Fig. 5, four peaks including C–C/C=C (284.6 eV), C–N (285.0 eV), C–O (286.2 eV), and C=N–C (289.2 eV) were also fitted in the C 1s XPS spectrum of the Co@CN-800 catalyst [43].

3.2. Reductive amination of benzaldehyde with nitrobenzene

Initially, the transfer hydrogenation of nitrobenzene was performed at 110°C , as it is the first step to realize the one-pot synthesis of secondary amines. Tetrahydrofuran (THF) was the best solvent to give 100% yield of aniline over the Co@CN-800 catalyst with a stoichiometric amount of formic acid (Table 3, Entries 1–8). *N*-Phenylformamide was also produced in toluene and water (Table 3, Entries 7 & 8), which was formed via a tandem reaction (Scheme S1). Increasing the formic acid amount to 6 equiv., *N*-phenylformamide was produced in a high yield of 92% (Table 3, Entry 9). The high selectivity of *N*-phenylformamide was due to the fact that the carbonyl group in *N*-phenylformamide was inert under the reaction conditions. Therefore, THF was used as the solvent for the one-pot reduction amination in the following experiments. The catalytic performance of Co@CN-800 was then compared with Co@CN-600 and Co@CN-900 (Table 3, Entries 6 vs 10 & 11) by the use of the same catalyst weight. The catalytic activity decreased in an order of Co@CN-800, Co@CN-600 and Co@CN-900. As dis-

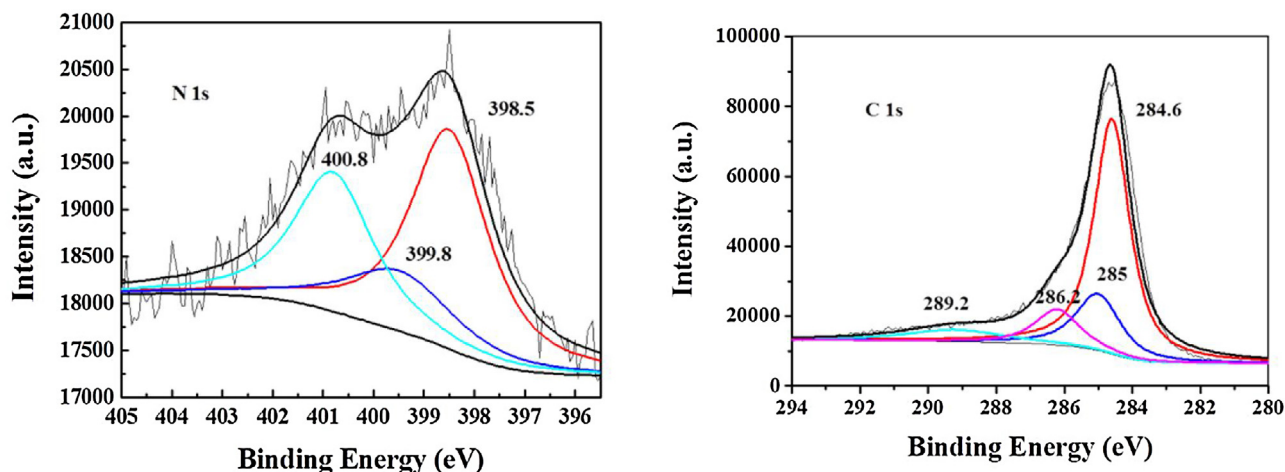


Fig. 5. The N 1s and C 1s XPS spectrum of the Co@CN-800 catalyst.

Table 3

The results of hydrogenation of nitrobenzene with formic acid.

Entry	Catalyst	Solvent	Time (h)	Con. (%)	Sel. A (%)	Sel. B (%)
1	Co@CN-800	Hexane	10	74	100	–
2	Co@CN-800	Ethanol	10	74	100	–
3	Co@CN-800	1,4-Dioxane	10	85	100	–
4	Co@CN-800	Ethyl acetate	10	94	100	–
5	Co@CN-800	DMF	10	96	100	–
6	Co@CN-800	THF	10	100	100	–
7	Co@CN-800	H ₂ O	10	80	83	17
8	Co@CN-800	Toluene	10	85	78	22
9 ^b	Co@CN-800	Toluene	12	100	8	92
10	Co@CN-600	THF	10	89	100	–
11	Co@CN-900	THF	10	78	100	–
12	Co@CN-800-Air	THF	10	0	–	–

^a Reaction conditions: nitrobenzene (1 mmol), solvent (10 mL), catalyst (40 mg), formic acid (3 mmol) and temperature (110 °C).

^b 6 mmol formic acid was used.

cussed later, both nitrogen and Co nanoparticles were found to be important for this reaction. The Co nanoparticles were the active sites for the transfer hydrogenation reaction with formic acid, which depended on the reaction rate. The nitrogen atoms acted as Lewis base to combine with the H⁺, and thus promoted the transfer hydrogenation. The Co@CN-800 catalyst had higher cobalt content than Co@CN-600, and thus had a higher reaction rate. Similarly, the Co@CN-600 catalyst showed a higher catalytic activity than the Co@CN-900 catalyst (Table 3, Entries 10 vs 11). These results suggested that Co nanoparticles played the main role in the activity of the CN@Co-T catalysts. As XPS results confirmed that some metallic Co in the surface of Co@CN-600, Co@CN-800 and Co@CN-900 was oxidized to the cobalt oxides. In order to determine the cobalt oxides whether had the catalytic activity towards the transfer hydrogenation of nitrobenzene with formic acid. We have compared the catalytic activity of Co@CN-800 and Co@CN-800-Air under the identical conditions, and it was found that Co@CN-800-Air was inactive (Table 3, Entry 12). These results indicated that the oxidation cobalt was not the active sites.

In addition, the treatment of the formic acid in THF at 110 °C was also conducted in the presence of the catalyst. It was noted that the pressure of the reactor remained constant during the reaction process, suggesting that no gas was formed during reaction process. On the other hand, the gas component after reaction was also analysed by gas chromatography, and no H₂ was detected. These

above results suggested that H₂ generated from the decomposition of formic acid was excluded.

Then the reductive amination of benzaldehyde with nitrobenzene was evaluated as a model reaction for the one-pot synthesis of secondary amines. In our study, aldehydes were excessive to nitro compounds (molar ratio = 2) in order to promote the condensation step of the aldehyde with primary amines (Table S1). The reason we used excessive aldehyde was that the condensation product of imine can reversely transform into primary amines and benzaldehyde with water in the presence of formic acid (98 wt.%). The reaction was firstly conducted at 110 °C over the Co@CN-800 catalyst. Unfortunately, the major product was the intermediate *N*-benzylideneaniline with a selectivity of 86.3% at full nitrobenzene conversion after 10 h, suggesting that the transfer hydrogenation of C=N bond was much more difficult than the nitro group (Fig. 6). Thus, reactions were then performed at higher temperatures. As shown in Fig. 6, the transfer hydrogenation of *N*-benzylideneaniline (C=N bond) was greatly accelerated with the increase of the reaction temperature, especially at low temperature range. High *N*-benzylideneaniline yields of 95.7% and 97.2% were produced at 170 and 190 °C after 10 h, respectively.

The transfer hydrogenation of nitrobenzene was performed at 170 °C without the catalyst, and no conversion was observed. The results suggested that the nitrobenzene reduction was a metal-catalyzed reaction even at a high temperature of 170 °C.

Table 4
Substrate scope of the developed catalytic system^a.

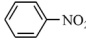
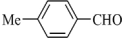
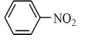

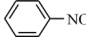
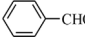
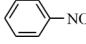
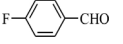
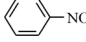
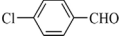
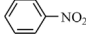
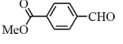
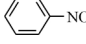
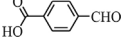
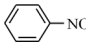
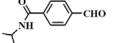
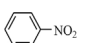
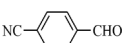
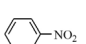
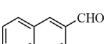
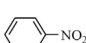
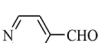
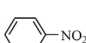
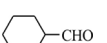
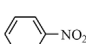
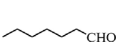
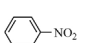
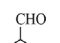
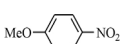
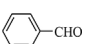
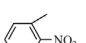
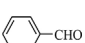
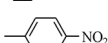
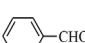
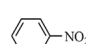
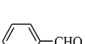

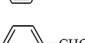
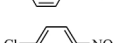
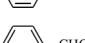
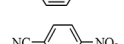
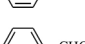

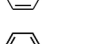
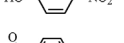
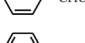
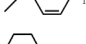
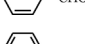
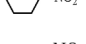
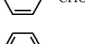
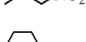
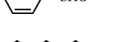
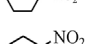
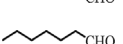
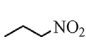
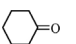
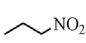
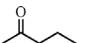
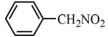
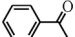
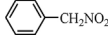
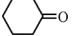
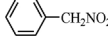
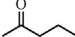
$\text{R-NO}_2 + \text{R}'\text{-}\overset{\text{O}}{\parallel}\text{C-R}'' \longrightarrow \text{R}'\text{-}\overset{\text{NHR}}{\text{CH}}\text{-R}''$						
Entry	Nitro compounds	Carbonyl compounds	Time (h)	Con. (%) ^b	Sel. (%) ^b	Isolated yield (%)
1			10	100	98.0	93
2			10	100	97.0	90
3			10	100	95.7	89
4			14	100	96.5	94
5			14	100	97.0	92
6			15	100	96.3	94
7			18	100	90.4	–
8			18	100	95.5	91
9			14	100	96.4	92
10			15	100	92.2	–
11 ^b			10	100	91.0	–
12			10	100	95.0	90
13			10	100	>99	91
14			10	100	>99	93
15			10	100	>99	95
16			15	100	91.0	–
17			10	100	92.2	–
18			10	100	90.8	–
19			12	100	93.8	–
20			12	100	95.3	89
21			12	100	>99	93
22			20	100	92.2	–
23			14	100	95.6	88
24			14	100	92.4	–
25			20	100	93.0	–
26			10	100	94.6	–
27			10	100	94.5	–
28			10	100	91.0	–
29			10	100	89.6	–

Table 4 (Continued)

$\text{R-NO}_2 + \text{R}'\text{-C(=O)-R}'' \longrightarrow \text{R}'\text{-C(=O)-NHR}''$						
Entry	Nitro compounds	Carbonyl compounds	Time (h)	Con. (%) ^b	Sel. (%) ^b	Isolated yield (%)
30			14	100	91.0	–
31			14	100	92.4	–
32			14	100	94.0	–

^a Reaction conditions: nitrobenzene (1 mmol), aldehydes or ketons (2 mmol), Co@CN-800 (40 mg), THF (10 mL), formic acid (4.5 mmol) and 170 °C; The conversion and the selectivity of the intermediate and the product were calculated based on nitro compounds.

^b The reaction was performed at 190 °C.

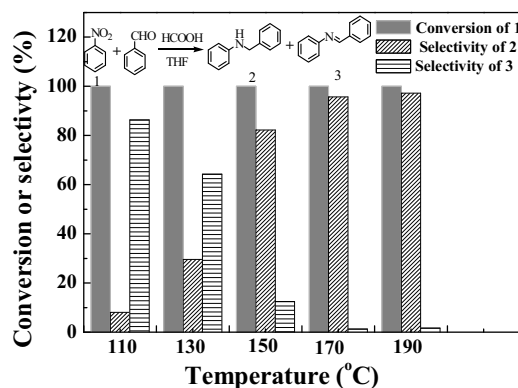


Fig. 6. Reductive amination of benzaldehyde with nitrobenzene at different temperatures. Reaction conditions: benzaldehyde (2 mmol), nitrobenzene (1 mmol), the Co@CN-800 catalyst (40 mg), THF (10 mL), HCOOH (4.5 mmol) and time (10 h). The conversion and the selectivity of the intermediate and the product were calculated based on nitrobenzene.

We also performed the transfer hydrogenation of the intermediate of *N*-benzylideneaniline without the catalyst, which produced a conversion of 13.8% after 1 h with the selectivity of 100% to *N*-benzylaniline. The hydrogenation of *N*-benzylideneaniline into *N*-benzylaniline with formic acid was called a Leuckart-Wallach reaction, which was finished via a six-member ring as the intermediate. However, the conversion of *N*-benzylideneaniline increased to 43.5% with the selectivity of 100% to *N*-benzylaniline over the Co@CN-800 catalyst. These results suggested that the Co@CN-800 catalyst also greatly promoted the second transfer hydrogenation step of *N*-benzylideneaniline.

3.3. Substrate scope

The scope of the developed method was then explored. Firstly, various aldehydes were reductively aminated with nitrobenzene. Aromatic aldehydes reacted smoothly with nitrobenzene to give secondary amines with excellent yields at 170 °C (Table 4, Entries 1–9). However, aromatic aldehydes with electron-withdrawing groups showed lower activity (Table 4, Entries 1–3 vs 4–9), which required a longer reaction time to get high yields. Similarly, nitroarenes with electron-withdrawing groups also showed lower activity than the counterparts with electron-withdrawing groups (Table 4, Entries 19–23). Substrates with electron-withdrawing groups resulted in a lower electronic density of C=N bonds and nitro groups, which were less active than those with electron-donating groups. 2-Naphthaldehyde as a fused-ring aromatic aldehyde was also successfully transformed into the secondary amine with a yield of 92.2% after 15 h (Table 4, Entry 10). Moreover, the catalytic system was also effective for the less-active heterocyclic, linear and

cyclic aldehydes or nitro compounds as the substrates under certain reaction conditions (Table 4, Entries 11–14, 24–25). It was even effective for reactions with the substrates that were both non-aromatic (Table 4, Entries 26–29).

The steric hindrance greatly affected the activity of the substrates. For example, the reaction with the ortho-isomer compared to para- or meta-isomers was slower due to the steric effect (Table 4, Entries 16–18). This phenomenon was much more obvious with aromatic ketons as the substrates. The reductive amination of acetophenone with nitrobenzene only produced aniline. That was also the reason for the selective reductive amination of 4-nitroacetophenone with benzylaldehyde (Table 4, Entry 23). The absence of the self-reductive amination of 4-nitroacetophenone was due to the steric hindrance of the keton group, and the 4-aminoacetophenone from the hydrogenation of 4-nitroacetophenone selective underwent the condensation with benzylaldehyde. While the one-pot reaction of the acetophenone with nitrophenylmethane yielded the corresponding secondary amine with high yield (Table 4, Entry 30). In addition, the reductive amination of nitrophenylmethane with linear and cyclic ketons also underwent smoothly. More importantly, this catalytic process was tolerant with other reducible groups including halogen (Table 4, Entries 4, 5, 19 & 20), esters (Table 4, Entry 6), carboxylic acids (Table 4, Entry 7), amides (Table 4, Entry 8), nitrile (Table 4, Entries 9 & 21), phenol (Table 4, Entry 22). In addition, we have also tried to isolate some products of the secondary amines by flash chromatography, which were detected by GC chromatography. As shown in Table 4, it was pleased that the isolated yields were also satisfactory, which were closed to the GC yields.

3.4. Kinetic and mechanism studies

Fig. 7 recorded the products distribution during the reaction process of the reductive amination of benzylaldehyde with nitrobenzene at 150 °C. Nitrobenzene was completely consumed within 2 h, while it required 16 h at to get the highest yield of *N*-benzylaniline, suggesting the transfer hydrogenation of the intermediate *N*-benzylideneaniline (C=N bond) was the rate determining step. Furthermore, the reaction rate constant *k* for the transfer hydrogenation of nitrobenzene at 110 °C was calculated to be 0.0082 min^{−1}, while that was 0.0010 min^{−1} for the transfer hydrogenation of *N*-benzylideneaniline at 110 °C, respectively (Fig. 8). The kinetic data again confirmed that the transfer hydrogenation of imines was the rate determining step.

To investigate the transfer hydrogenation mechanism with formic acid over the Co@CN-800 catalyst, the reduction of nitrobenzene was used as the model reaction. So far, the transfer hydrogenation reactions with formic acid were generally performed with base as the additive [27,28]. However, no base was required in our catalytic system. We assumed that the nitrogen

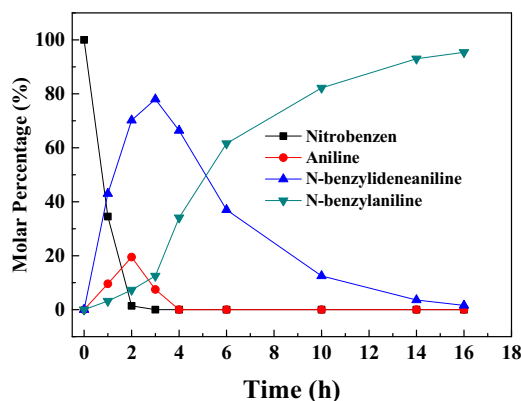


Fig. 7. The products distribution during the reductive amination of benzylaldehyde with nitrobenzene. Reaction conditions: Nitrobenzene (1 mmol), benzylaldehyde (2 mmol), Co@CN-800 (40 mg), THF (10 mL), formic acid (4.5 mmol) and 150 °C. The data was calculated based on nitrobenzene.

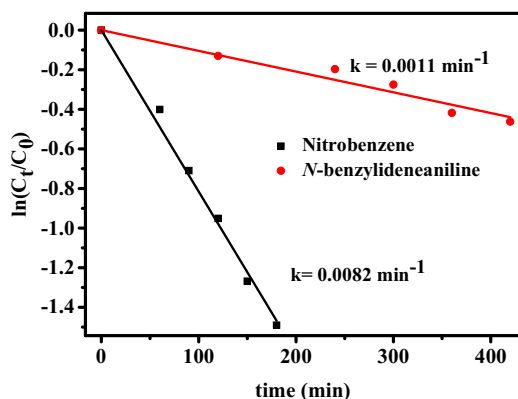
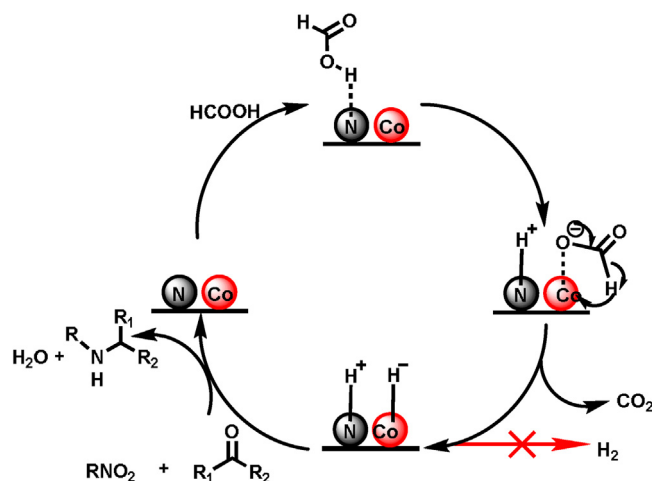


Fig. 8. Compare the transfer hydrogenation rate of nitrobenzene and the intermediate *N*-benzylideneaniline. Reaction conditions: Nitrobenzene (1 mmol) or *N*-benzylideneaniline, Co@CN-800 (40 mg), THF (10 mL), formic acid (10 mmol) and 110 °C.

atoms in the Co@CN-800 catalyst should act as a base. To confirm this assumption, the reaction was also carried out with 3 equiv. of formic acid and 3 equiv. of H_3PO_4 . No conversion was observed again (Table S2, Entry 3). H_3PO_4 with a stronger acidity more readily neutralized the nitrogen atoms to form NH^+ , thus deactivated the Co@CN-800 catalyst. These above results suggested that the nitrogen atoms and Co nanoparticles played synergetic roles in the transfer hydrogenation. According to the above analysis, a plausible mechanism was proposed for the one-pot reductive amination (Scheme 3). Firstly, the electronegative nitrogen atoms in the Co@CN-800 catalyst capture the H^+ from formic acid to generate NH^+ , and cobalt-formate species are also formed. The formate anions tended to coordinate on the surface of the Co nanoparticles, as the electron negative formate anions can coordinated with the empty d orbitals [44]. In fact, other researchers also reported that metal-formate species were present during the decomposition of formic acid into H_2 [45,46], when nitrogen in the catalyst or the addition of organic base was used. Then, the release of CO_2 molecule generates the cobalt-hydride species (Co-H^-). The combination of Co-H^- with NH^+ to generate H_2 was not observed in our system, and the possible reason should be due to the intrinsic lower activity of Co nanoparticles as compared with noble metal catalysts [46]. The process of the generation of NH^+ and Co-H^- resembles as the heterolytic cleavage of H_2 , in which nitrogen atoms in the catalysts or an additional base promoted the heterolytic cleavage [46,47]. For example, Bullock and co-workers proposed the nitrogen atoms in the Fe complex served as the basic sites to promote the heterolytic



Scheme 3. Proposed mechanism for the reductive amination by transfer hydrogenation.

Table 5

The transfer hydrogenation of nitrobenzene with D-substituted formic acid over the Co@CN-800 catalyst.

Entry	Formic acid	Reaction rate ($\mu\text{mol min}^{-1} \text{ g}_{\text{catalyst}}^{-1}$)	KIE ^b
1	HCOOH	64.6	–
2	DCOOD	60.1	1.07
3	DCCOH	12.8	4.06

^a Reaction conditions: nitrobenzene (1 mmol), THF (10 mL), Co@CN-800 catalyst (40 mg), temperature (110 °C), 1 h and nitrogen atmosphere (10 bar).

^b KIE = rate(entry 1)/rate(entry n); n = 2–3.

cleavage of H_2 to generate the protic $\text{N-H}^{\delta+}$ and hydridic $\text{Fe-H}^{\delta-}$ part [47]. Thus, the generation of NH^+ and Co-H^- was reasonable according to the above analysis and the control experiments, which were the active species for the transfer hydrogenation of nitro groups and $\text{C}=\text{N}$ bonds (Scheme 3). In fact, a proton (H^+) and a hydride (H^-) were often reported for the reduction of polar bonds such as $\text{C}=\text{O}$ and $\text{C}=\text{N}$ bonds [48], while the homolytic cleavage of H_2 was suitable for the reduction of non-polar bonds such as $\text{C}=\text{C}$ and $\text{C}\equiv\text{N}$ bonds [49,50]. Obviously, the proposed mechanism reveals that the generation of Co-H^- should be the rate-limiting step for the transfer hydrogenation. The deuterium-labelling studies (Table 5) revealed that a larger kinetic isotope effect (KIE) of 4.06 was observed using DCCOH for the reduction of nitrobenzene, while the KIE was only 1.07 by the use of DCOOD, in agreement with the dehydrogenative activation of formic acid over supported Au catalysts [45]. The deuterium-labelling studies further confirmed the proposed mechanism was reasonable.

3.5. Recycling of the Co@CN-800 catalyst

Finally, the stability of the Co@CN-800 catalyst was also studied. After reaction, the catalyst could be facily separated with an external magnet (Fig. S8). As depicted in Fig. 9, *N*-benzylaniline yield in first run with fresh catalyst was almost the same as the subsequent seven runs with the spent catalyst, evidently suggesting that the Co@CN-800 catalyst was highly stable. Notably, the cobalt content in the reaction solution was below the ICP detection limit. TEM images also indicated that Co nanoparticles embedded in the carbon structure were intact (Fig. S9). Co@CN-800 with high stability should be attributed to the fact that Co nanoparticles were embedded in the carbon layer, and the catalyst was prepared by acid-washing, thus the deactivi by aggregation and leach that were often observed with supported catalysts can be avoided.

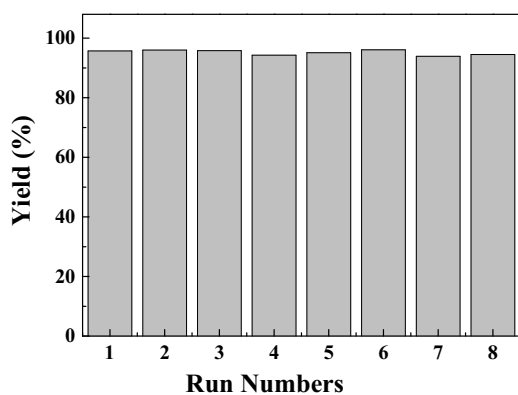


Fig. 9. The results of the recycling experiments of the Co@CN-800 catalyst. Reaction conditions: Nitrobenzene (1 mmol), benzaldehyde (2 mmol), Co@CN-800 catalyst (40 mg), THF (10 mL), formic acid (4.5 mmol), 170 °C and 10 h.

4. Conclusions

In conclusion, mesoporous nitrogen-doped carbon-embedded Co nanoparticles (CN@Co-800) were prepared via the hard template method. This inexpensive and easily handled cobalt catalyst facilitates the one-pot synthesis secondary amines for the first time via the reductive amination of carbonyl compounds with nitro compounds with formic acid as the hydrogen donor. Secondary amines were produced in excellent yields with structure diversely carbonyl compounds and nitro compounds. Moreover, this protocol was found to tolerate a wide range of functional groups, such as halogen, amides, esters, carboxylic acids, nitrile, and phenols. One of the distinct advantages is that the CTH reactions were performed with formic acid without base or other additives. Mechanism studies revealed that the nitrogen atoms served as a base to generate the Co-formate species, followed by the generation of a proton (H⁺) and a hydride (H[−]) to reduce the nitro groups and C=N bonds. Kinetic studies revealed that the CTH of the imines was the rate determining step. The CTH of the carbonyl groups was inert under our reaction conditions, and that should be the reason for the high selectivity of secondary amines. Compared with the previously reported methods, our developed catalytic system evidently holds multiple advantages such as cost effectiveness (using nonprecious metals as catalyst), environmental safety (using renewable formic acid without additives), simplicity (facile magnetic separation of the catalyst), high stability and a broad substrate scope. Hence, the proposed catalytic system holds great potential in practical applications for the synthesis of secondary amines via reductive amination of carbonyl compounds with nitro compounds.

Acknowledgement

The Project was supported by National Natural Science Foundation of China (No. 21203252).

Appendix A. Supplementary data

Supplementary data associated with this article can be found, in the online version, at <http://dx.doi.org/10.1016/j.apcatb.2017.04.026>.

References

- [1] P.N. Rylander, *Catalytic Hydrogenation in Organic Syntheses*, Academic Press, New York, 1979.
- [2] S. Nishimura, *Handbook of Heterogeneous Catalytic Hydrogenation for Organic Synthesis*, Wiley, New York, 2001.
- [3] R.M. Bullock, Abundant metals give precious hydrogenation performance, *Science* 342 (2013) 1054–1055.
- [4] A.M. Smith, R. Whyman, Review of methods for the catalytic hydrogenation of carboxamides, *Chem. Rev.* 114 (2014) 5477–5510.
- [5] N. Ono, *The Nitro Group in Organic Synthesis*, John Wiley & Sons, 2003.
- [6] A. Corma, P. Serna, Chemoselective hydrogenation of nitro compounds with supported gold catalysts, *Science* 313 (2006) 332–334.
- [7] A. Noschese, A. Buonerba, P. Canton, S. Milione, C. Capacchione, A. Grassi, Highly efficient and selective reduction of nitroarenes into anilines catalyzed by gold nanoparticles incarcerated in a nanoporous polymer matrix: role of the polymeric support and insight into the reaction mechanism, *J. Catal.* 340 (2016) 30–40.
- [8] J. Feng, S. Handa, F. Gallou, B.H. Lipshutz, Safe and selective nitro group reductions catalyzed by sustainable and recyclable Fe/ppm Pd nanoparticles in water at room temperature, *Angew. Chem. Int. Ed.* 55 (2016) 8979–8983.
- [9] H. Yang, S.J. Bradley, A. Chan, G.I. Waterhouse, T. Nann, P.E. Kruger, S.G. Telfer, Catalytically active bimetallic nanoparticles supported on porous carbon capsules derived from metal-organic framework composites, *J. Am. Chem. Soc.* 138 (2016) 11872–11881.
- [10] E.W. Baxter, A.B. Reitz, Reductive aminations of carbonyl compounds with borohydride and borane reducing agents, *Org. React.* (2004) 1–714.
- [11] R.N. Salvatore, C.H. Yoon, K.W. Jung, Synthesis of secondary amines, *Tetrahedron* 57 (2001) 7785–7811.
- [12] D.S. Surry, S.L. Buchwald, Biaryl phosphane ligands in palladium-catalyzed amination, *Angew. Chem. Int. Ed.* 47 (2008) 6338–6361.
- [13] J.F. Hartwig, Evolution of a fourth generation catalyst for the amination and thioetherification of aryl halides, *Acc. Chem. Res.* 41 (2008) 1534–1544.
- [14] S.V. Ley, A.W. Thomas, Modern synthetic methods for copper-mediated C(aryl)–O, C(aryl)–N, and C(aryl)–S bond formation, *Angew. Chem. Int. Ed.* 42 (2003) 5400–5449.
- [15] D.S. Surry, S.L. Buchwald, Diamine ligands in copper-catalyzed reactions, *Chem. Sci.* 1 (2010) 13–31.
- [16] M.H.S. Hamid, C.L. Allen, G.W. Lamb, A.C. Maxwell, H.C. Maytum, A.J. Watson, J.M. Williams, Ruthenium-catalyzed N-alkylation of amines and sulfonamides using borrowing hydrogen methodology, *J. Am. Chem. Soc.* 131 (2009) 1766–1774.
- [17] R.V. Jagadeesh, T. Stemmler, A.-E. Surkus, H. Junge, K. Junge, M. Beller, Hydrogenation using iron oxide-based nanocatalysts for the synthesis of amines, *Nat. Protoc.* 10 (2015) 548–557.
- [18] L. Li, Z. Niu, S. Cai, Y. Zhi, H. Li, H. Rong, L. Liu, L. Liu, W. He, Y. Li, A PdAg bimetallic nanocatalyst for selective reductive amination of nitroarenes, *Chem. Commun.* 49 (2013) 6843–6845.
- [19] L. Hu, X. Cao, D. Ge, H. Hong, Z. Guo, L. Chen, X. Sun, J. Tang, J. Zheng, J. Lu, Ultrathin platinum nanowire catalysts for direct C–N coupling of carbonyls with aromatic nitro compounds under 1 bar of hydrogen, *Chem. Eur. J.* 17 (2011) 14283–14287.
- [20] M. Pintado-Sierra, A.M. Rasero-Almansa, A. Corma, M. Iglesias, F. Sánchez, Bifunctional iridium-(2-aminoterephthalate)-Zr-MOF chemoselective catalyst for the synthesis of secondary amines by one-pot three-step cascade reaction, *J. Catal.* 299 (2013) 137–145.
- [21] T. Stemmler, F.A. Westerhaus, A.-E. Surkus, M.-M. Pohl, K. Junge, M. Beller, General and selective reductive amination of carbonyl compounds using a core-shell structured Co₃O₄/NGr@C catalyst, *Green Chem.* 16 (2014) 4535–4540.
- [22] E.A. Artiukha, A.L. Nuzhdin, G.A. Bukhtiyarova, S.Y. Zaytsev, P.E. Plyusnin, Y.V. Shubin, V.I. Bukhtiyarov, One-pot reductive amination of aldehydes with nitroarenes over an Au/Al₂O₃ catalyst in a continuous flow reactor, *Catal. Sci. Technol.* 5 (2015) 4741–4745.
- [23] D. Wang, D. Astruc, The golden age of transfer hydrogenation, *Chem. Rev.* 115 (2015) 6621–6686.
- [24] D. Chusov, B. List, Reductive amination without an external hydrogen source, *Angew. Chem. Int. Ed.* 53 (2014) 5199–5201.
- [25] J.W. Park, Y.K. Chung, Hydrogen-free cobalt-rhodium heterobimetallic nanoparticle-catalyzed reductive amination of aldehydes and ketones with amines and nitroarenes in the presence of carbon monoxide and water, *ACS Catal.* 5 (2015) 4846–4850.
- [26] Q. Zhang, S.-S. Li, M.-M. Zhu, Y.-M. Liu, H.-Y. He, Y. Cao, Direct reductive amination of aldehydes with nitroarenes using bio-renewable formic acid as a hydrogen source, *Green Chem.* 18 (2016) 2507–2513.
- [27] E.E. Drinkel, R.R. Campedelli, A.M. Manfredi, H.D. Fiedler, F. Nome, Zwitterionic-surfactant-stabilized palladium nanoparticles as catalysts in the hydrogen transfer reductive amination of benzaldehydes, *J. Org. Chem.* 79 (2014) 2574–2579.
- [28] C. Wang, A. Pettman, J. Bacsá, J. Xiao, A versatile catalyst for reductive amination by transfer hydrogenation, *Angew. Chem. Int. Ed.* 49 (2010) 7548–7552.
- [29] H.H. Khoo, W.L. Ee, V. Isoni, Bio-chemicals from lignocellulose feedstock: sustainability, LCA and the green conundrum, *Green Chem.* 18 (2016) 1912–1922.
- [30] K.H. Lim, H. Kim, Nitrogen-doped carbon catalysts derived from ionic liquids in the presence of transition metals for the oxygen reduction reaction, *Appl. Catal. B: Environ.* 158 (2014) 355–360.
- [31] D. Singh, I.I. Soykal, J. Tian, D. von Deak, J. King, J.T. Miller, U.S. Ozkan, In situ characterization of the growth of CN_x carbon nano-structures as oxygen reduction reaction catalysts, *J. Catal.* 304 (2013) 100–111.

- [32] K. Yokoyama, S. Yokoyama, Y. Sato, K. Hirano, S. Hashiguchi, K. Motomiya, H. Ohta, H. Takahashi, K. Tohji, Y. Sato, Efficiency and long-term durability of a nitrogen-doped single-walled carbon nanotube electrocatalyst synthesized by defluorination-assisted nanotube-substitution for oxygen reduction reaction, *J. Mater. Chem. A* 4 (2016) 9184–9195.
- [33] Y. Liang, Y. Li, H. Wang, J. Zhou, J. Wang, T. Regier, H. Dai, Co_3O_4 nanocrystals on graphene as a synergistic catalyst for oxygen reduction reaction, *Nat. Mater.* 10 (2016) 780–786.
- [34] F.A. Westerhaus, R.V. Jagadeesh, G. Wienhöfer, M.-M. Pohl, J. Radnik, A.-E. Surkus, J. Rabeah, K. Junge, H. Junge, M. Nielsen, Heterogenized cobalt oxide catalysts for nitroarene reduction by pyrolysis of molecularly defined complexes, *Nat. Chem.* 5 (2013) 537–543.
- [35] C.V. Nguyen, Y.-T. Liao, T.-C. Kang, J.E. Chen, T. Yoshikawa, Y. Nakasaka, T. Masuda, K.C.-W. Wu, A metal-free, high nitrogen-doped nanoporous graphitic carbon catalyst for an effective aerobic HMF-to-FDCA conversion, *Green Chem.* 18 (2016) 5957–5961.
- [36] W. Zhong, H.-L. Liu, C.-H. Bai, S.-J. Liao, Y.-W. Li, Base-free oxidation of alcohols to esters at room temperature and atmospheric conditions using nanoscale Co-based catalysts, *ACS Catal.* 5 (2015) 1850–1856.
- [37] R.V. Jagadeesh, D. Banerjee, P.B. Arockiam, H. Junge, K. Junge, M.M. Pohl, A. Brückner, M. Beller, Highly selective transfer hydrogenation of functionalised nitroarenes using cobalt-based nanocatalysts, *Green Chem.* 17 (2015) 898–902.
- [38] K. Wang, R. Wang, H. Li, H. Wang, X. Mao, V. Linkov, S. Ji, N-doped carbon encapsulated Co_3O_4 nanoparticles as a synergistic catalyst for oxygen reduction reaction in acidic media, *Int. J. Hydrogen Energy* 40 (2015) 3875–3882.
- [39] Z.-S. Wu, L. Chen, J. Liu, K. Parvez, H. Liang, J. Shu, H. Sachdev, R. Graf, X. Feng, K. Müllen, High-performance electrocatalysts for oxygen reduction derived from cobalt porphyrin-based conjugated mesoporous polymers, *Adv. Mater.* 26 (2014) 1450–1455.
- [40] Y. Yang, L. Jia, B. Hou, D. Li, J. Wang, Y. Sun, The correlation of interfacial interaction and catalytic performance of N-doped mesoporous carbon supported cobalt nanoparticles for Fischer-Tropsch synthesis, *J. Phys. Chem. C* 118 (2013) 268–277.
- [41] Y. Yao, L.-L. Gu, W. Jiang, H.C. Sun, Q. Su, J. Zhao, W.-J. Ji, C.-T. Au, Enhanced low temperature CO oxidation by pretreatment: specialty of the Au- Co_3O_4 oxide interfacial structures, *Catal. Sci. Technol.* 6 (2016) 2349–2360.
- [42] W.-N. Wang, Y. Itoh, I.W. Lenggoro, K. Okuyama, Nickel and nickel oxide nanoparticles prepared from nickel nitrate hexahydrate by a low pressure spray pyrolysis, *Mater. Sci. Eng. B* 111 (2004) 69–76.
- [43] S.-H. Liu, Y.-F. Dong, Z.-Y. Wang, H.-W. Huang, Z.-B. Zhao, J.-S. Qiu, Towards efficient electrocatalysts for oxygen reduction by doping cobalt into graphene-supported graphitic carbon nitride, *J. Mater. Chem. A* 3 (2015) 19657–19661.
- [44] J. Tan, J. Cui, X. Cui, T. Deng, X. Li, Y. Zhu, Y. Li, Graphene-modified Ru nanocatalyst for low-temperature hydrogenation of carbonyl groups, *ACS Catal.* 5 (2015) 7379–7384.
- [45] Q.-Y. Bi, X.-L. Du, Y.M. Liu, Y. Cao, H.Y. He, K.-N. Fan, Efficient subnanometric gold-catalyzed hydrogen generation via formic acid decomposition under ambient conditions, *J. Am. Chem. Soc.* 134 (2012) 8926–8933.
- [46] Q. Liu, X. Yang, Y. Huang, S. Xu, X. Su, X. Pan, J. Xu, A. Wang, C. Liang, X. Wang, et al., A Schiff base modified gold catalyst for green and efficient H_2 production from formic acid, *Energy Environ. Sci.* 8 (2015) 3204–3207.
- [47] T. Liu, X. Wang, C. Hoffmann, D.L. DuBois, R.M. Bullock, Heterolytic cleavage of hydrogen by an iron hydrogenase model: an Fe-H \cdots H-N dihydrogen bond characterized by neutron diffraction, *Angew. Chem. Int. Ed.* 53 (2014) 5300–5304.
- [48] M. Devillard, R. Brousses, K. Miqueu, G. Bouhadir, D. Bourissou, A stable but highly reactive phosphine-coordinated borenium: metal-free dihydrogen activation and alkyne 1,2-carbaboration, *Angew. Chem. Int. Ed.* 54 (2015) 5722–5726.
- [49] R. Noyori, Asymmetric catalysis: science and opportunities (Nobel Lecture), *Angew. Chem. Int. Ed.* 41 (2002) 2008–2022.
- [50] A.A. Mikhailine, M.I. Maishan, A.J. Lough, R.H. Morris, The mechanism of efficient asymmetric transfer hydrogenation of acetophenone using an iron (II) complex containing an (S, S)- $\text{Ph}_2\text{PCH}_2\text{CH}(\text{NCHPh})\text{CHPhN}(\text{CHCH}_2\text{PPh}_2)$ ligand: partial ligand reduction is the key, *J. Am. Chem. Soc.* 134 (2012) 12266–12280.